High power density proton-exchange membrane fuel cells

Oliver J. Murphy, G. Duncan Hitchens and David J. Manko
Lynntech, Inc., 7610 Eastmark Drive, Suite 105, College Station, TX 77840 (USA)

Abstract

Proton-exchange membrane (PEM) fuel cells use a perfluorosulfonic acid solid polymer film as an electrolyte which simplifies water and electrolyte management. Their thin electrolyte layers give efficient systems of low weight, and their materials of construction show extremely long laboratory lifetimes. Their high reliability and their suitability for use in a microgravity environment makes them particularly attractive as a substitute for batteries in satellites utilizing high power, high energy-density electrochemical energy storage systems. In this investigation, the Dow experimental PEM (XUS-13204.10) and unsupported high platinum loading electrodes yielded very high power densities, of the order of 2.5 W cm^{-2}. A platinum black loading of 5 mg cm^{-2} was found to be optimum. On extending the three-dimensional reaction zone of fuel cell electrodes by impregnating solid-polymer electrolyte into the electrode structures, Nafion® was found to give better performance than the Dow experimental PEM. The depth of penetration of the solid polymer electrolyte into electrode structures was 50–70% of the thickness of the platinum-catalyzed active layer. However, the degree of platinum utilization was only 16.6% and the roughness factor of a typical electrode was 274.

Introduction

There is increasing interest in the development of fuel cell systems as power sources in space, on land and for marine applications [1–3]. Since fuel cells bring about the direct conversion of stored chemical energy to electrical energy without the intermediate generation of thermal energy, they are not limited by the Carnot cycle, unlike heat engines [4]. Thus, energy-conversion efficiencies for fuel cell systems (45–65%) are generally a factor of 2 higher than those for heat engines, e.g., diesel generators. Although considerable advances have been made in fuel cell systems over the past three decades [5, 6], they are still considered as an emerging technology. However, for manned spacecraft applications (Gemini, Apollo and Space Shuttle Orbiter), relatively small (1–12 kW) and highly reliable fuel cell power plants have been fabricated and used successfully. Similarly, for terrestrial electrical power generation, relatively large systems (40 kW–11 MW) have been built and demonstrated to be viable candidates for commercial power generation [7].

Traditionally, satellite energy storage has been provided by nickel/cadmium batteries and, more recently, by rechargeable nickel/hydrogen batteries [8], where the primary power source is solar photovoltaic panels. However, with increasing satellite applications, and the associated growing demand for electrical energy storage, in particular, for systems having high peak power outputs, has lead to a search for alternatives to rechargeable aqueous-based battery systems [8]. Operating conditions with respect to

SSDI 0378-7753(93)01778-G

the charge regime and cycle life of satellite power sources have become much more demanding, in particular, for long-lived, low earth orbit (LEO) satellites in equatorial orbit [9]. For such an application, the number of cycles required of an electrochemical energy storage system is 5840 per year, or over 50 000 for a ten-year satellite lifetime. This extremely high cycle life has led to the consideration of lightweight, efficient, high power density, regenerative fuel cells for such satellite applications [8, 10].

High power densities, and high energy conversion efficiencies, are a prerequisite for the development of lightweight, small-volume and low-cost fuel cell systems having high specific energies (Wh/kg) and high energy densities (Wh/l). At present, the only fuel cell systems that have the capability of achieving high power densities (>1 W cm^{-2}) are the proton-exchange membrane (PEM) and the alkaline fuel cell (AFC) systems [11, 12]. Of these, the PEM system is the leading candidate fuel cell-based power source for demanding satellite applications. The attractiveness of this fuel cell system stems from a number of advantageous characteristics that it possesses, compared with AFC systems. These include: (i) low-temperature operation; (ii) cold start-up capability; (iii) negligible electrolyte management problems, since it uses a proton-exchange polymer membrane as an electrolyte; (iv) infinite life on open-circuit stand; (v) higher reliability; (vi) toleration of high reactant gas pressure differentials across the PEM electrolyte layer, and (vii) ease of thermal and fluid management. Because of the attainment of high power density and high energy conversion efficiency, together with the CO_2-rejecting nature of the strongly acidic PEM electrolyte layer, this fuel cell system readily satisfies the requirement of a dual-use fuel cell technology, e.g., as the power source for electric vehicles where air, rather than oxygen, is used as the oxidant feed gas.

Research and development areas presently being addressed by many research groups, in order to make PEM fuel cells cost competitive and more effective in meeting various mission requirements, involve optimizing the structure, chemical composition and configuration of fuel cell components [13–17]. These include: (i) electrode structures (platinum-based catalyst loadings and thicknesses of gas diffusion and active layers) [13, 18]; (ii) PEM electrolyte material (thickness, conductivity, stability and mechanical characteristics) [11, 13, 17]; (iii) preparation of membrane and electrode (M&E) assemblies (hot-pressed membranes and gas diffusion electrodes, cast-active layers on membranes in physical contact with gas-diffusion electrodes and electrodeposited noble metal catalysts in the outer layers of PEM-impregnated gas-diffusion electrodes) [13, 15, 19]; (iv) lightweight, readily mass produced, bipolar plates, cell frames and gasket materials [20], and (v) thermal and water management [16].

In the present investigation, various proton-exchange membrane materials, together with unsupported, high platinum loading electrodes (1–10 mg Pt cm^{-2}), were used as the basic cell components for carrying out performance evaluations in 5 cm^2 active area single-cell test fixtures. To increase the utilization of expensive platinum electrocatalysts, electrode structures were impregnated with a solubilized form of various proton-exchange membrane materials. Membrane and electrode assemblies were prepared by a proprietary hot-pressing procedure. Humidified oxygen and hydrogen gases at various pressures were used as reactants. Performance characteristics (V–i curves) were recorded at various cell operating conditions (temperature and reactant gas pressures). Using representative M&E assemblies, a cyclic voltammetric technique was used to measure the degree of platinum catalyst utilization in porous gas-diffusion electrodes. Also, energy dispersive spectroscopy (EDS) was applied to the cross sections of tested M&E assemblies, in order to determine the thickness of active electrode layers and the depth of penetration of solubilized PEM material into electrode structures.

Experimental

Electrodes and proton-exchange membranes

High surface area, pure-platinum black electrocatalyst materials were used for both the hydrogen and oxygen electrodes. The geometric area of each electrode was 5 cm^2. Commercially available (Johnson–Matthey, Inc.) fuel cell gas diffusion electrodes, fabricated using unsupported platinum black (surface area of 35–50 $m^2\ g^{-1}$), with platinum loadings of either 1, 2.5, 5 or 10 mg cm^{-2} were used.

Three proton-exchange membrane materials, two from Du Pont and one from Dow Chemical Company, were investigated. Of these, only Nafion® 117 from Du Pont is commercially available. The others, Nafion® 115 and the Dow experimental membrane (XUS-13204.10) were made available in small quantities for experimental purposes. The acid membranes consist of a thin film of perfluorinated sulfonic acid polymer material that possesses good chemical and thermal stabilities [21, 22]. The structural formula for these cation-exchange membranes is given in Fig. 1. Both Nafion® 117 and Nafion® 115 have equivalent weights of 1100 and thicknesses in the dry state of 175 μm and 125 μm, respectively. The Dow experimental membrane has an equivalent weight of approximately 800, a thickness in the wet state of 125 μm and a conductivity of approximately 0.12 $\Omega^{-1}\ cm^{-1}$, as measured with an a.c. bridge [23].

Before being used, PEM materials were washed in various solutions to remove trace organic and inorganic contaminants. The purification procedure involved boiling the proton-exchange membranes in a 10 vol.% aqueous H_2O_2 (30 vol.%) solution for one hour, followed by boiling for one hour in pure water and subsequently boiling for a second hour in a fresh sample of pure water. Membranes were then removed and boiled for one hour in 0.5 M H_2SO_4, followed by boiling for one hour each in two different samples of pure water. On completing the purification procedure, membrane specimens were stored in the last sample of washwater at room temperature prior to use.

A 5 wt.% Nafion solution in a mixture of lower aliphatic alcohols and 10% water was obtained from Aldrich Chemical Company. Portions of this solution (or a similar in-house prepared solution of the Dow PEM material) were brush-coated onto the catalyzed surfaces of fuel cell electrodes. On allowing the first coat to dry in air for a few minutes, a second coat was then applied in a similar fashion. Afterward, the PEM-impregnated electrodes were placed in an oven at 80 °C and allowed to dry for 45 min in an air atmosphere. From the difference in weight before and after impregnation, PEM loadings (approximately 0.6 mg cm^{-2}) within the catalyzed electrode structures were determined.

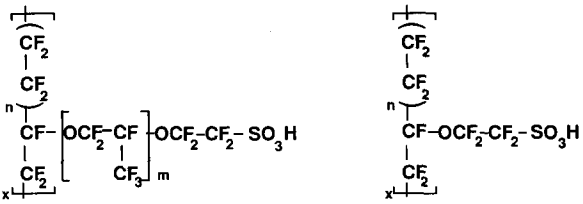

Fig. 1. Structural formula for proton-exchange membranes: (a) structure of Du Pont's Nafion® $n = 6.6$ and $m = 1$, and (b) structure of Dow experimental membrane $n = 3.6$–10.

PEM-impregnated electrodes were bonded onto both sides of purified proton-exchange membranes, using a proprietary hot-pressing procedure. Pressed M&Es were immediately removed from the hot press and mounted in a test fuel cell fixture.

Single-cell test fuel cells

Test fuel cell fixtures were fabricated using machined graphite blocks, having rib-channel patterns on one side, which facilitated the distribution of humidified gases to the porous gas-diffusion electrodes, as well as providing current collection from the electrodes. The active cell area, represented by the rib-channel patterns, was 5 cm^2. A M&E assembly, which is the principal component of a cell, was obtained on pressing porous electrode materials onto both sides of a proton-exchange membrane, using a proprietary method. Teflon-coated fiberglass gasket materials, placed on both sides of the membrane, provided sealing on bolting the cell components together. Copper endplates enabled test cell fixtures to be bolted together, and electrical cartridge heaters inserted into the walls of the copper plates allowed various operating cell temperatures to be selected.

After allowing 24 h to condition a new M&E assembly in a test fuel cell fixture under predetermined gas pressures (usually 0 psi hydrogen and 0 psi oxygen) and a temperature of 50 °C, the performance characteristics of a cell were determined. This involved placing an electronic load, set to operate in the constant load mode, between the terminals of a cell. Performance characteristics (V–i curves) were then recorded at various operating conditions of a cell (temperature and pressure). On completing performance characterizations for some of the test cells, the oxygen gas inlet was removed from the cathode compartment and replaced by an inert gas, e.g., argon. The cathode compartment was then purged overnight with argon, and cyclic voltammetric profiles for the oxygen electrode were subsequently recorded at a scan rate of 50 mV s^{-1} between the potential limits of hydrogen- and oxygen-gas evolution at a cell temperature of 50 °C with hydrogen gas at 1 atm flowing over the anode and reference electrodes, and argon gas at a pressure of 1 atm flowing over the cathode. The latter profiles were recorded using an EG&G PAR Instruments model 362 scanning potentiostat, in conjunction with a Yokogawa model 3025 x-y recorder.

Test station hardware

Fuel cell test stations used in this investigation had: (i) microprocessor control of hydrogen and oxygen gas temperatures entering the fuel cell; (ii) control of gas pressures from atmospheric to 200 psi; (iii) flow meters for the control and measurements of gas flow rates; (iv) electronic loads with a maximum capability of 300 W, and (v) a data acquisition system, with appropriate interfacing for the automated collection and processing of data. An important component of each test station was an attached temperature-controlled environment chamber that housed the test fuel cell fixture and the hydrogen and oxygen gas humidification vessels. The temperature of the controlled environment chamber could be raised or lowered on activating an electrical heating pad placed at the bottom of the chamber. Appropriate electrical connections to components within the chamber were made by isolated electrical feedthroughs, mounted on the walls of the chamber.

Results and discussion

Nature of PEM electrolyte material on the performance of M&E assemblies

Since ohmic overpotentials are largely determined by the thickness and by the conductivity of proton-exchange membranes, the performance of M&E assemblies using

membrane materials thinner than Nafion® 117 (e.g., Nafion® 115) and alternative membranes having the same thickness as Nafion® 115 but at least a factor of 2 higher in conductivity (e.g., Dow experimental membrane, XUS-13204.10) were evaluated. The more highly conducting Dow PEM also possesses better water retention characteristics than Nafion®.

Using unsupported high platinum loading electrodes (5 mg Pt cm^{-2}) and segments of Nafion 117®, Nafion® 115 and the Dow experimental membrane, M&E assemblies were prepared. *V–i* profiles for the resulting assemblies, tested at a fuel cell temperature of 95 °C with hydrogen/oxygen reactant gas pressures of 30 psi/40 psi, are presented in Fig. 2. A considerable improvement in PEM fuel cell performance was obtained on using the Dow experimental proton-exchange membrane, as compared with Nafion® proton-exchange membranes.

In the absence of mass transport overpotentials, and taking the hydrogen/oxidation reaction to be kinetically fast, the three *V–i* profiles presented in Fig. 2 may be expressed by [24, 25]:

$$V = V_0 - b \log i - R_i i \quad (1)$$

$$V_0 = V_r + b \log i_0 \quad (2)$$

where V_r is the thermodynamic reversible potential for the fuel cell reaction, i_0 and b are the exchange-current density and Tafel slope for the oxygen-reduction reaction and R_i is the differential resistance of the cell. When activation overpotential (primarily due to the oxygen-reduction reaction) and ohmic overpotential are the major sources of power loss, the data points corresponding to these regions in the *V–i* profiles can be fitted to eqn. (1), and the parameters V_0, b and R_i extracted using the method of least squares fit. Excellent agreement between the experimental data points and simulated *V–i* profiles from the curve fitting was obtained up to current densities where mass-transport effects became noticeable. The values of V_0, b and R_i for the three M&E assemblies, represented by the *V–i* profiles presented in Fig. 2, are summarized in Table 1.

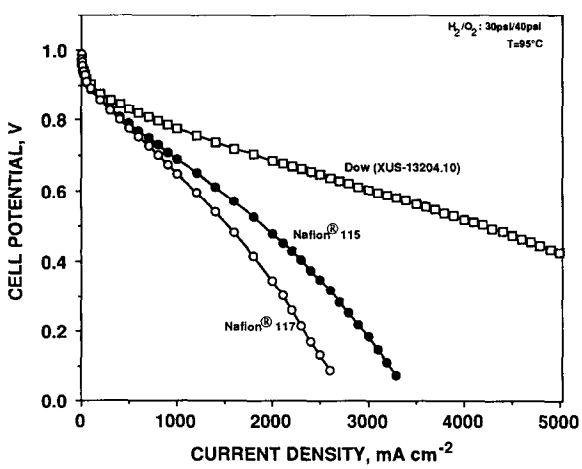

Fig. 2. Fuel cell potential–current density profiles for M&E assemblies containing Nafion® 117, Nafion® 115 and the Dow PEM.

TABLE 1

Values of V_0, b and R_i for M&E assemblies containing either Nafion® 117, Nafion® 115 or the Dow membrane (XUS-13204.10) as polymer electrolyte

Polymer electrolyte	Reactants	Reactant pressures (psi)	Fuel cell temperature (°C)	V_0 (V)	b (V decade^{-1})	R_i (Ω cm^2)
Nafion® 117	H_2/O_2	30/40	95	1.012	0.052	0.208
Nafion® 115	H_2/O_2	30/40	95	0.995	0.044	0.176
Dow membrane	H_2/O_2	30/40	95	1.013	0.053	0.075

The values for V_0, which correspond to the cell potential at a current density of 1 mA cm^{-2}, are similar for the three M&E assemblies. The values for the Tafel slope, b, are close to those reported by other investigators [26]. The interesting result from the Table is given by the values for R_i, which decrease in an expected manner on taking into account the physicochemical characteristics of the Nafion® and Dow membrane materials [23, 27]. Based on these values of R_i, the exceptionally good performance obtained from the M&E assembly containing the Dow membrane can be readily understood in terms of low ohmic overpotentials.

The value of 0.075 Ω cm^2 for the M&E assembly containing the Dow membrane consists of the resistance across the membrane itself and contact resistances between other components in the test fuel cell fixture. In the absence of a Dow PEM, the contact resistances for the identical fuel cell fixture, and similar electrodes were measured at 95 °C and yielded a value of 0.032 Ω cm^2. Thus, the resistance across the PEM itself was 0.043 Ω cm^2. On taking the reported value for the specific resistance of the Dow PEM, 8 Ω cm [23] and the actual measured thickness (45 μm) of the Dow PEM in the hot-pressed M&E assembly yields a membrane resistance of 0.036 Ω cm^2. Thus, using the developed proprietary hot-pressing procedure for the preparation of M&E assemblies, ohmic losses across M&E assemblies approach their theoretically limiting values.

V–i profiles for an M&E assembly (Dow PEM and unsupported, high platinum-loading electrodes – 5 mg Pt cm^{-2}), fabricated using the proprietary hot-pressing procedure and tested using a fuel cell temperature of 95 °C and hydrogen/oxygen gas pressures of 30 psi/40 psi, 60 psi/70 psi and 160 psi/160 psi, are presented in Fig. 3. As expected, increasing gas pressures gave rise to better fuel cell performance due to the effect of pressure on electrochemical reaction rates.

Variations of power density with cell potential and with current density for this M&E assembly tested at a fuel cell temperature of 95 °C with hydrogen/oxygen gas pressures of 160 psi/160 psi, using both humidified and dry oxygen gas are presented in Figs. 4(a) and (b), respectively. It can be seen from the Figs. that the fuel cell performed surprisingly well on dry oxygen gas and may be able to function satisfactorily in this manner, at least for short periods of time, e.g., under pulse power conditions. More importantly, it is apparent from the data presented in Fig. 4 that extremely high power densities of the order of 2.5 W cm^{-2} were obtained at a cell potential of 0.48 V and a current density of 5.1 A cm^{-2}.

Impact of electrode structure on the performance of M&E assemblies

To maximize electrocatalyst utilization in PEM fuel cells, previous researchers [26, 28] impregnated catalyzed electrode structures with solubilized Nafion® PEM

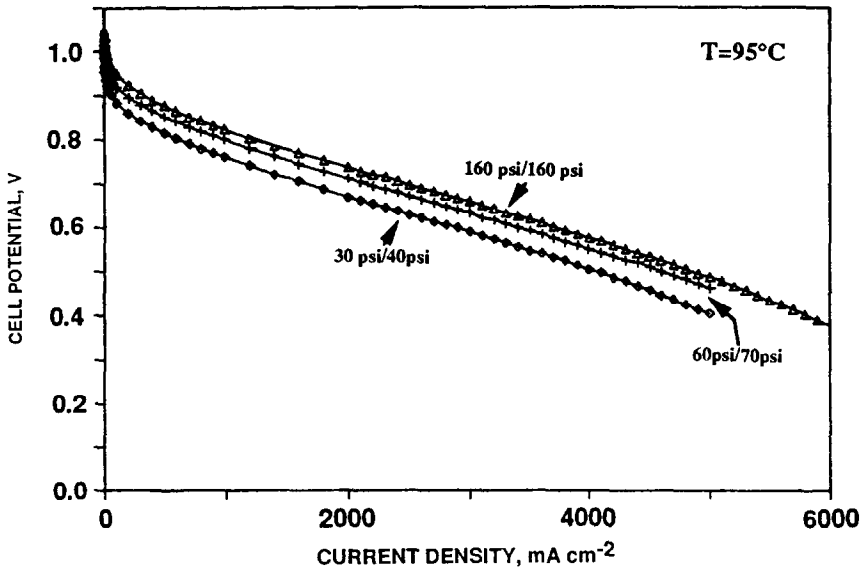

Fig. 3. Fuel cell potential–current density profiles for a Dow PEM-based M&E assembly tested at various hydrogen/oxygen gas pressures.

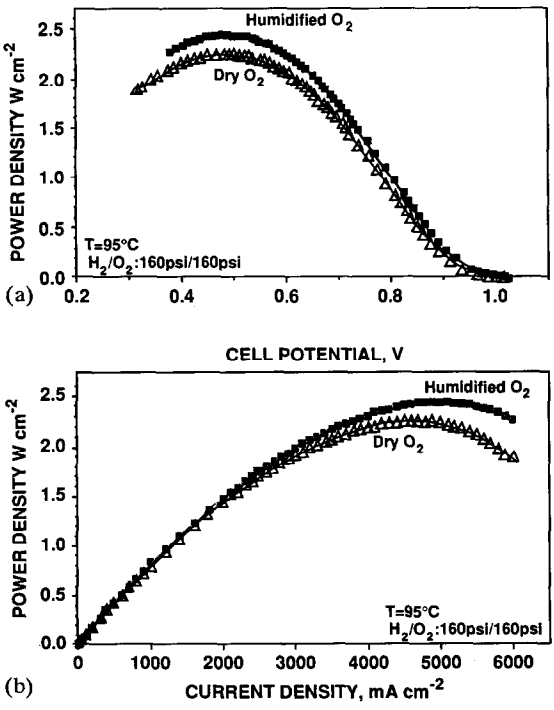

Fig. 4. Variation of power density: (a) with cell potential, and (b) with current density for a PEM fuel cell supplied with humidified hydrogen gas and humidified or dry oxygen gas.

material. This treatment was found to enhance the three-dimensional nature of the active catalyzed layers of fuel cell electrodes and was observed to give rise to a reduction in activation and mass-transport overpotentials [13, 25, 26]. Because of the improved fuel cell performance obtained on using the Dow experimental PEM as the solid electrolyte film, it was decided to investigate if further improvements in fuel cell performance could be obtained if solubilized Dow membrane solution was impregnated into the catalyzed electrode layers instead of the Nafion® solution. Thus, M&E assemblies were fabricated using the Dow experimental PEM as electrolyte and unsupported, high platinum-loading electrodes (5 mg Pt cm^{-2}). However, for one M&E assembly, the electrodes were impregnated with the commercially available Nafion® solution, while the second M&E assembly was constructed using identical electrodes but impregnated with in-house prepared Dow membrane solution [29, 30].

V–i profiles for the two similar M&E assemblies tested using a fuel cell temperature of 95 °C and hydrogen/oxygen gas pressures of 100 psi/100 psi are presented in Fig. 5. It can be seen from the Fig. that the Nafion®-impregnated electrodes gave better performance than the corresponding Dow-impregnated electrodes. This was also observed from data derived from other similar M&E assemblies. This unexpected result may be due to the fact that the lower equivalent weight of the Dow experimental membrane with its associated higher sulfonic acid group content, giving rise to increased water retention in the membrane, brings about flooding within the electrode structures, which impedes the access of reactant gases to platinum catalyst sites. However, the higher $-CF_2-$ content of Nafion® compared with the Dow PEM (cf., Fig. 1) facilitates a greater solubility of dissolved oxygen in the Nafion®-impregnated PEM electrolyte material [31]. The higher localized concentration of dissolved oxygen at platinum particle/PEM electrolyte interfaces within electrode structures can support higher oxygen-reduction reaction rates accounting for the trend observed. Hence, while the

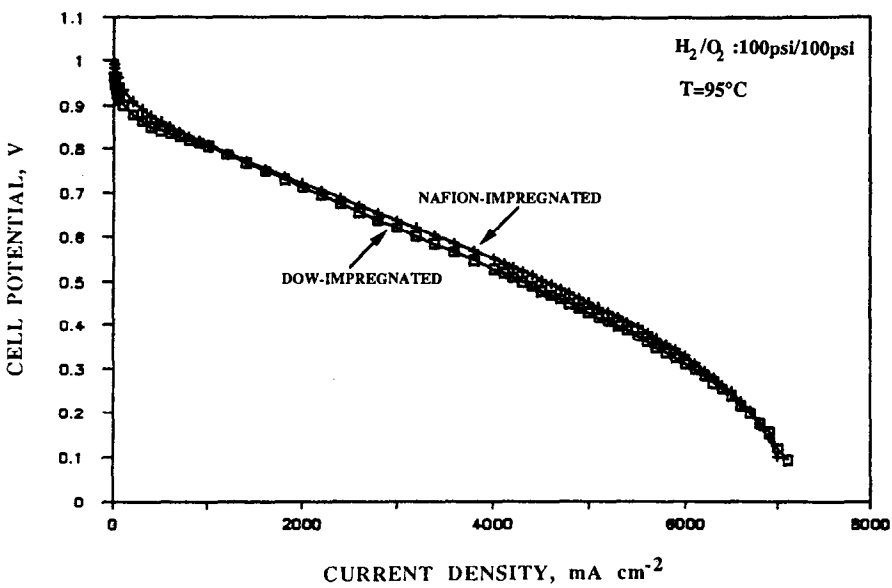

Fig. 5. Fuel cell potential–current density profiles for M&E assemblies containing Nafion-impregnated or Dow-impregnated high platinum-loading electrodes.

characteristics of the Dow PEM are most suitable when it is used as the proton-exchange membrane itself, they may not be as appropriate as Nafion® for impregnation within electrode structures. Thus, it seems that the best combination for an optimized M&E assembly is the use of the Dow experimental PEM as the electrolyte layer and dissolved Nafion® as the electrolyte material to be used for impregnating catalyzed electrodes, so as to increase the three-dimensional character of fuel cell electrodes.

On operating PEM fuel cells at high power densities, most of the electrochemical reactions, giving rise to high cell currents, will occur near the front surface of the catalyzed electrodes. A simple analysis of electrode pore models shows that high IR drops within the length of pores dictates that most of the current is localized in the outer catalyzed layers of electrodes. Hence, to achieve high power densities, it is advantageous to localize a large fraction of the electrocatalyst material in the outer layers of fuel cell electrodes. Therefore, platinum electrocatalyst loading would be expected to have a significant effect on the performance of PEM fuel cells.

To investigate the effect of platinum electrocatalyst loading on PEM fuel cell performance, a number of M&E assemblies were fabricated using the Dow experimental PEM and Nafion®-impregnated, unsupported platinum electrodes with loadings of 1, 2.5, 5 or 10 mg Pt cm^{-2}. *V–i* profiles for the resulting assemblies, tested using a fuel cell temperature of 95 °C and hydrogen/oxygen gas pressures of 100 psi/100 psi, are presented in Fig. 6. Fuel cell performance was observed to increase with increasing platinum catalyst loading, reaching a maximum at a loading of 5 mg Pt cm^{-2}. This can be more clearly seen in the variation of power density with cell potential and with current density, shown in Fig. 7, for these assemblies. The dependence of maximum power density on platinum catalyst loading was in the order: 5 mg cm^{-2}> 10 mg cm^{-2}>2.5 mg cm^{-2}>1 mg cm^{-2}. Relatively thick platinum-catalyzed active layers, as found in electrodes having a platinum-loading of 10 mg cm^{-2}, may impede

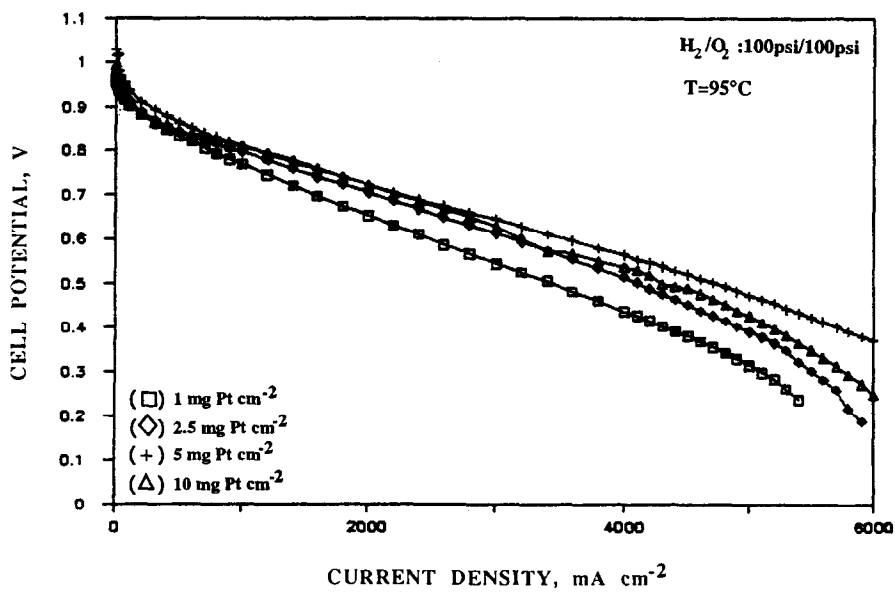

Fig. 6. Fuel cell potential–current density profiles for M&E assemblies containing high platinum-loading electrodes.

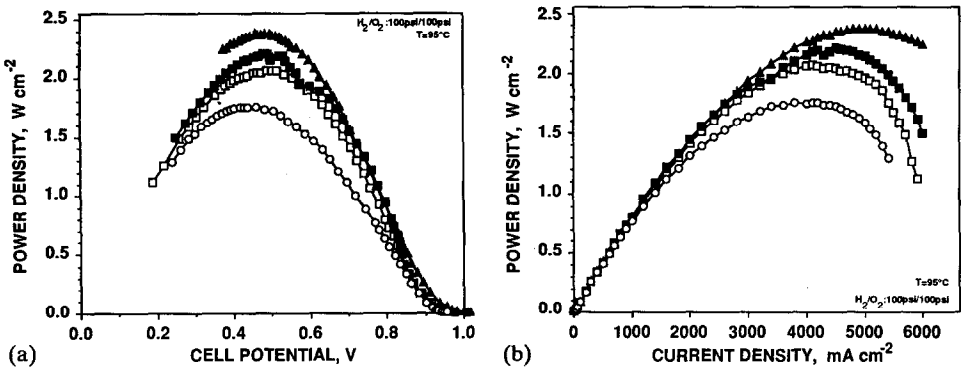

Fig. 7. Variation of power density: (a) with cell potential, and (b) with current density for a PEM fuel cell supplied with humidified hydrogen and oxygen gases. M&E assemblies consisted of the Dow experimental membrane and unsupported high platinum-loading electrodes: (○) 1 mg Pt cm^{-2}; (□) 2.5 mg Pt cm^{-2}; (▲) 5.0 mg Pt cm^{-2}, and (■) 10.0 mg Pt cm^{-2}.

the access of dissolved PEM material into the electrode structures or introduce mass-transport overpotentials, which hinder high fuel cell performance. The behavior of the M&E assembly with the highest platinum-loading electrodes at high current densities (cf., Fig. 6) supports these conclusions.

In the case of unsupported, high surface area platinum black catalyzed electrodes, active layer thicknesses corresponding to a platinum loading of 5 mg cm^{-2} are optimum for PEM fuel cells yielding the highest performance. For aerospace applications where high performance and reliability are of the highest priority, the cost associated with the platinum, approximately $200 per kW at a current density of 1 A cm^{-2} [19], can be justified. However, for terrestrial applications, e.g., fuel cell power sources for electric vehicles, this cost figure is too high and carbon-supported, low platinum loading electrodes will have to be used.

Scanning electron microscopy and energy dispersive spectroscopy of M&E assemblies

Scanning electron micrographs (SEM) at various magnifications of the cross section of an M&E assembly, fabricated using Nafion®-impregnated, unsupported, high platinum loading electrodes (5 mg Pt cm^{-2}) and the Dow experimental proton exchange membrane (XUS-13204.10) are presented in Fig. 8. The fibers in the weaves of the carbon cloth backing can be readily seen in Fig. 8(a). The bonding between the membrane and the electrocatalyst layers appears to be excellent, and no degradation was observed after completing a short-duration lifetime test (240 h). The cross section of the M&E assembly, shown in the SEM given in Fig. 8(b), is centered on the interface between the proton-exchange membrane and the catalyzed layers of one electrode. Some of the locations along the cross section, where energy dispersive spectroscopy (EDS) elemental analyses were performed, are numbered on the micrograph. Exposure of the electron beam spot on the proton-exchange membrane during EDS data collection brought about decomposition of the PEM polymer material (Fig. 8(b)).

The three key layers of the M&E assembly, namely, the gas-diffusion layer, the active platinum-catalyzed layer and the PEM electrolyte film, were analyzed using EDS. Representative EDSs for each of these layers are presented in Fig. 9. The gas-diffusion layer (Fig. 9(a)) shows high-intensity elemental carbon and fluorine signals, arising from the Teflon-bonded, high surface area carbon powder material used in

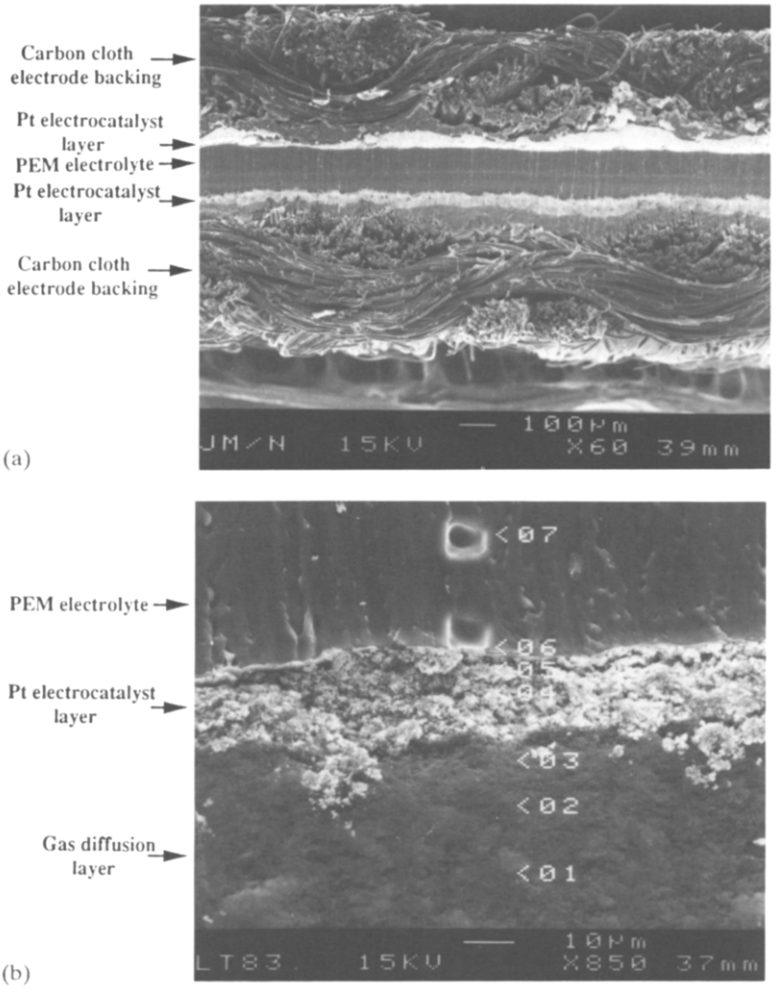

Fig. 8. Scanning electron micrographs of the cross section of an M&E assembly fabricated using Nafion-impregnated unsupported high platinum-loading electrodes and Dow experimental PEM.

fabricating this layer. The weak elemental platinum signal observed is probably due to carry-over of platinum particles from the active layer on slicing the M&E assembly. The EDS for the active platinum electrocatalyst layer (Fig. 9(b)) is dominated by a high-intensity elemental platinum signal, as expected. Also, in this Fig., weak signals from carbon and fluorine (associated with Teflon bonding of the platinum electrocatalyst particles) and sulfur are to be noted; the latter is probably associated with Nafion® impregnated into the active platinum-catalyzed layer. In the EDS derived from the PEM electrolyte film (Fig. 9(c)), high-intensity signals were obtained, corresponding to carbon, fluorine and sulfur. This is in agreement with a proton-exchange membrane consisting of a perfluorosulfonic acid polymer material. No elemental platinum dissolved into the membrane during fuel cell operation, as evidenced by the lack of a platinum signal.

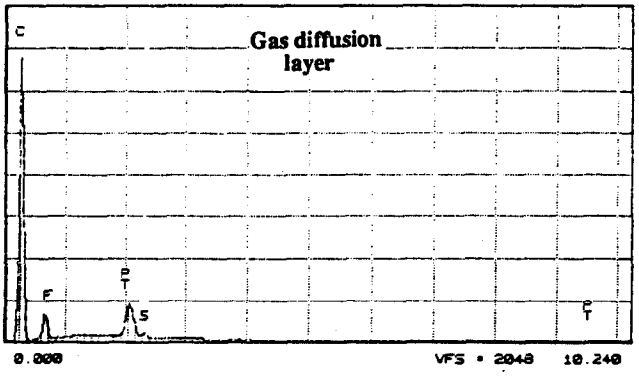

(a)

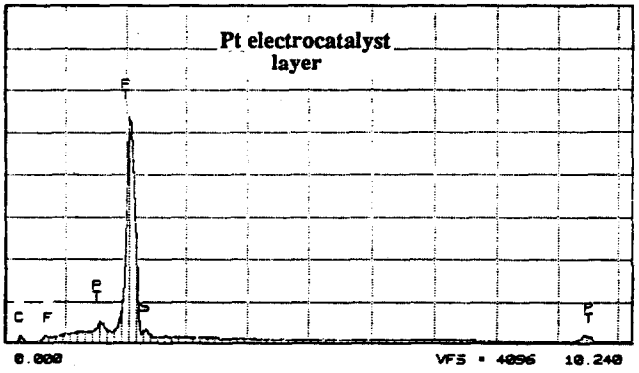

(b)

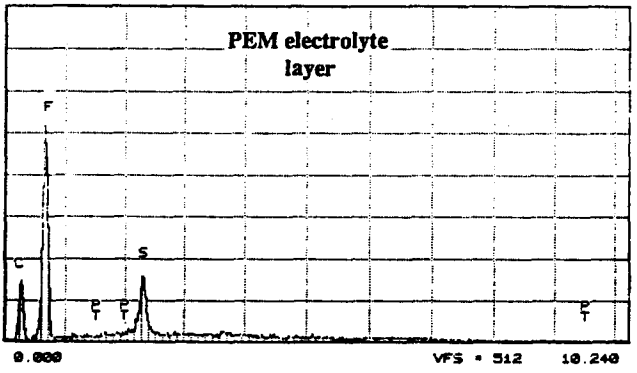

(c)

Fig. 9. Energy dispersive spectrographs taken at three different locations along the cross section of an M&E assembly fabricated using unsupported high platinum-loading electrodes and Dow experimental membrane.

Elemental peak height ratios as a function of distance across the cross section of the M&E assembly, shown in the electron micrograph presented in Fig. 8(b), are given in Fig. 10. The profile derived from the Pt/C elemental peak height ratios shows

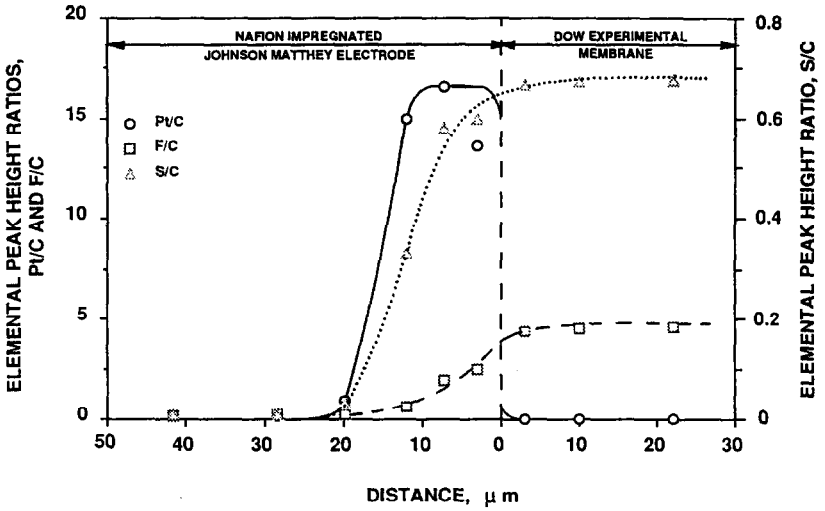

Fig. 10. Elemental peak height ratios as a function of distance along the cross section of an M&E assembly fabricated using unsupported high platinum-loading electrodes and Dow experimental PEM.

that the thickness of the platinum-catalyzed active layer is approximately 15–20 μm. Examination of the profiles associated with S/C and F/C elemental peak height ratios, given in Fig. 10, demonstrate that the impregnated Nafion® does not penetrate the entire thickness of the unsupported platinum-catalyzed active layer. A rough estimate of the Nafion®-penetration depth is of the order of 50–70% of the thickness of the platinum-catalyzed active layer. This depth of penetration of solubilized Nafion® into the platinum-catalyzed active layer is likely to be sufficient for PEM fuel cell operation at high power densities (cf., Figs. 3 and 4). However, for high energy conversion efficiencies at lower current densities, new methods which facilitate greater penetration of solubilized Nafion® into active catalyzed layers need to be developed.

Electrocatalyst utilizations and roughness factors for unsupported, high platinum-loading fuel cell electrodes

The charge associated with the formation of a hydrogen monolayer or the removal of a monolayer of oxide film, measured with the cyclic voltammetric technique, was used to estimate the degree of platinum utilization and the roughness factor of unsupported, high platinum loading (5 mg Pt cm^{-2}) fuel cell electrodes. Cyclic voltammetric profiles recorded for Nafion®-impregnated, unsupported platinum black electrodes in test fuel cell fixtures are given in Fig. 11. The voltammetric profiles are similar to those obtained for smooth platinum in aqueous acid solutions [32]. The poorly resolved hydrogen adsorption and desorption regions, the double-layer region and the oxide film formation and reduction regions are easily discernible. From the voltammetric charge associated with either the monolayer oxide film reduction peak or the adsorbed hydrogen monolayer region, information can be derived concerning the electrochemically active surface area and the degree of platinum electrocatalyst utilization under typical fuel cell operating conditions. The relevant data are presented in Table 2.

It can be seen from the Table that satisfactory agreement between the adsorbed hydrogen monolayer charge and the oxide film reduction charge was obtained. From

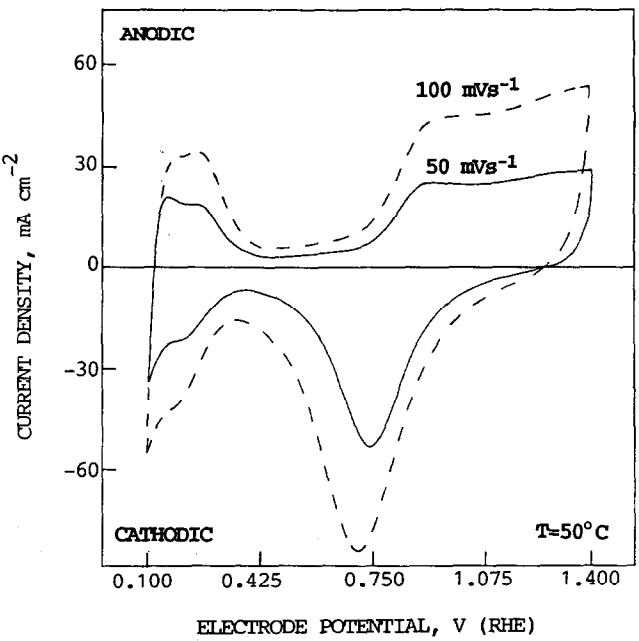

Fig. 11. Cyclic voltammograms for an M&E assembly fabricated using Nafion-impregnated unsupported high platinum-loading electrodes (5 mg Pt cm^{-2}) and Nafion 117 PEM.

TABLE 2

Roughness factor and degree of platinum utilization for Nafion-impregnated unsupported high surface area platinum black-based fuel cell electrode

	Nafion-impregnated electrode[a]
Experimentally determined adsorbed hydrogen charge, $Q_{H,exptl.}$ (mC)	288
Experimentally determined oxide film reduction charge, $Q_{O,exptl.}$ (mC)	566
Experimentally determined electrochemically active surface area, E_{SA}, from $Q_{H,exptl.}$ (assuming 210 μC cm^{-2}) (cm^2)	1371
Calculated real surface area (assuming 85 Å diameter platinum particles (cm^2)	8250
Geometric surface area, G_{SA} (cm^2)	5
Surface roughness factor (ratio of experimentally determined electrochemically active surface area (E_{SA}) to geometric surface area (G_{SA}))	274
Calculated adsorbed hydrogen charge, $Q_{H,calc.}$ (assuming 85 Å diameter platinum particles) (mC)	1733
Degree of electrocatalyst utilization, $Q_{H,exptl.}/Q_{H,calc.}$ (%)	16.6

[a]Unsupported high surface area platinum black-based electrode with a platinum loading of 5 mg cm^{-2}.

the known platinum catalyst loading (5 mg Pt cm^{-2}) and assuming spherical platinum particles, 85 Å in diameter, a maximum electrochemically active surface area was estimated. For the unsupported, high platinum loading, oxygen electrode, comparison of the calculated and experimentally determined electrochemically active areas or adsorbed hydrogen charges indicate that the degree of platinum utilization was only 16.6% and that the roughness factor for this electrode was 274. Clearly, either some of the surface of the platinum particles are not in contact with the Nafion®-impregnated electrolyte material or not all of the surface is electrochemically active. The non-electrochemical EDS technique tends to overestimate the thickness of the platinum-catalyzed layer taking part in electrochemical reactions. Further investigations are necessary to resolve this issue.

Conclusions

1. To obtain high power densities in PEM fuel cells, activation, ohmic and mass-transport overpotentials were minimized by the use of optimized M&E assemblies.
2. The Dow experimental PEM (XUS-13204.10) gave much superior performance than Nafion® PEM materials, which are manufactured by Du Pont.
3. Extremely high power densities of the order of 2.5 W cm^{-2} were obtained at a cell potential of 0.48 V and a current density of 5.1 A cm^{-2} on using the Dow PEM and unsupported, high platinum-loading electrodes (5 mg Pt cm^{-2}).
4. Electrode structure factors, e.g., nature of the three-dimensional active catalyzed layer, electrocatalyst loading, etc., had a significant effect on PEM fuel cell performance, that is, in obtaining high power densities.
5. Elevated reactant gas pressures and fuel cell temperatures considerably enhanced fuel cell performance.
6. There was no evidence of deterioration or degradation in any of the tested M&E assemblies or other fuel cell components after completing fuel cell performance evaluations.

Acknowledgements

Proton-exchange membrane fuel cell research and development work performed at Lynntech, Inc., is supported by the US Air Force (Contract no. FO4611-90-C-0095) and by the US Navy (Contract no. N00024-91-C-4067). This support is gratefully acknowledged.

References

1 M. Warshay and P. Prokopius, *J. Power Sources, 29* (1990) 193.
2 R.A. Lemons, *J. Power Sources, 29* (1990) 251.
3 W.H. Kumm, *J. Power Sources, 29* (1990) 169.
4 J.O'M Bockris and S. Srinivasan, *Fuel Cells: Their Electrochemistry*, McGraw-Hill, New York, 1969.
5 S.S. Penner, *Energy (Oxford), 11* (1986) 1–229.
6 A.J. Appleby and F.R. Foulkes, *Fuel Cell Handbook*, Van Nostrand Reinhold, New York, 1989.

7 J.J. Hirschenhofer, *Mech. Eng.*, (Sept.) (1992) 82.
8 G. Halpert and A. Attia, in W.D. Jackson (ed.), *Proc. 24th Intersociety Energy Conversion Engineering Conf.*, Vol. 3, Institute of Electric and Electronic Engineers, New York, USA, 1989, p. 1429.
9 H.S. Lim and S.A. Verzwyvelt, *J. Power Sources, 22* (1988) 213.
10 A.J. Appleby, *J. Power Sources, 22* (1988) 377.
11 K. Prater, *J. Power Sources, 29* (1990) 239.
12 S. Srinivasan, *J. Electrochem. Soc., 136* (1989) 41C.
13 S. Srinivasan, O.A. Velev, A. Parthasarathy, D.J. Manko and A.J. Appleby, *J. Power Sources, 36* (1991) 299.
14 D.S. Watkins, K.W. Dircks and D.G. Epp, *US Patent No. 4 988 583* (Jan. 29, 1991).
15 M.S. Wilson and S. Gottesfeld, *J. Electrochem. Soc., 139* (1992) L28.
16 A.P. Meyer, in W.D. Jackson (ed.), *Proc. 24th Intersociety Energy Conversion Engineering Conf.*, Vol. 3, Institute of Electric and Electronic Engineers, New York, USA, 1989, p. 1619.
17 K. Straber, *Ber. Bunsenges. Phys. Chem., 94* (1990) 1000.
18 M.S. Wilson and S. Gottesfeld, *J. Appl. Electrochem., 22* (1992) 1.
19 E.J. Taylor, E.B. Anderson and N.R.K. Vilambi, *J. Electrochem. Soc., 139* (1992) L45.
20 S.M. Misiaszek, *Paper presented on Fuel Cell Developments at Energy Partners, West Palm Beach, FL, USA, Dec. 1992.*
21 A. Eisenberg and H.L. Yeager (eds.), *Perfluorinated Ionomer Membranes, ACS Symp. Ser., No. 180, 1982.*
22 Dow Chemical Company, *US Patent No. 4 417 969* (1983).
23 G.A. Eisman, *Ext. Abstr., Int. Seminar on Fuel Cell Technology and Applications, The Hague, Netherlands, Oct. 26–29, 1987,* p. 287.
24 M. Ratcliff, R.L. Posey, D.K. Johnson and H.L. Chum, *J. Electrochem. Soc., 132* (1985) 577.
25 S. Srinivasan, E.A. Ticianelli, C.R. Derouin and A. Redondo, *J. Power Sources, 22* (1988) 359.
26 E.A. Ticianelli, C.R. Derouin and S. Srinivasan, *J. Electroanal. Chem., 251* (1988) 275.
27 R.S. Yeo and H.L. Yeager, in B.E. Conway, R.E. White and J.O'M. Bockris (eds.), *Modern Aspects of Electrochemistry,* Vol. 16, Plenum, New York, 1985, pp. 437–504.
28 I.D. Raistrick, *US Patent No. 4 876 115* (Oct. 1989).
29 M.N. Szentirmay, L.F. Campbell and C.R. Martin, *Anal. Chem., 58* (1986) 661.
30 R.B. Moore and C.R. Martin, *Anal. Chem., 58* (1986) 2569.
31 S. Srinivasan, personal communication, Mar. 1993.
32 L.D. Burke and M.B.C. Roche, *J. Electroanal. Chem., 164* (1984) 315.